Near-field imaging of femtosecond laser ablated sub-λ/4 holes in lithium niobate

Airán Ródenas,[1,a)] Jorge Lamela,[1] Daniel Jaque,[1] Ginés Lifante,[1] Francisco Jaque,[1] Antonio García-Martín,[2] Guangyong Zhou,[3] and Min Gu[3]
[1]*Dept. de Física de Materiales, Universidad Autónoma de Madrid, Cantoblanco, 28047 Madrid, Spain*
[2]*Instituto de Microelectrónica de Madrid, IMM (CNM-CSIC), 28760 Tres Cantos, Spain*
[3]*Centre for Micro-Photonics and Centre for Ultrahigh-Bandwidth Devices for Optical Systems, Faculty of Engineering and Industrial Sciences, P.O. Box 218, Hawthorn, Victoria 3122, Australia*

(Received 19 August 2009; accepted 8 October 2009; published online 2 November 2009)

We report on the direct femtosecond laser ablation of sub-λ/4 (80–250 nm) holes in $LiNbO_3$ crystals and on its local near-field imaging. We show that the near-field transmission of holes can feature an attenuation of ~75% at hole central position, and a ~20% transmission enhancement at its sides. This high-contrast ring-shaped near-field distribution is found to be in agreement with simulations, suggesting the surface relief as the main contrast mechanism. © *2009 American Institute of Physics*. [doi:10.1063/1.3256219]

The possibility of creating controlled periodic nanostructures at the surface of ferroelectric nonlinear lithium niobate (LN) crystals is nowadays attracting much attention because of its numerous applications including the fabrication of two-dimensional (2D) photonic crystals,[1] microdiffraction elements,[2] 2D phononic crystals,[3] and focusing microstructures when combined with metallic coatings.[4] Among the different techniques capable of controlled surface structuring in LN crystals at the submicrometric scale (such as focused ion beam milling, ion beam enhanced etching, or mask assisted plasma etching), femtosecond laser ablation (FLA) is of special relevance because of its simplicity, reduced processing times, and absence of sample preparation requirements. The FLA technique is based on the combination of ultrashort laser pulses with tight focusing high numerical aperture (NA) optics. Precise material removal is produced by the photon-to-electron energy transfer via avalanche phenomena that leads to a well spatially confined deterministic optical breakdown. Under optimum conditions, this process can be induced in a spatial region with dimensions well below the irradiation wavelength ($\lambda_{FLA} \sim 800$ nm, in most of the cases). In the particular case of LN, surface holes with a $\lambda_{FLA}/2$ (400 nm) diameter have been already demonstrated by using standard NA=0.5 optics.[5] Nevertheless, for most of the above mentioned applications (especially those involving visible light control) reduced hole sizes are required. The possibility of using high-NA (NA>1) optics has been already demonstrated in several materials (including glasses and organic self-assembled monolayers),[6,7] but its potential application in LN crystals for beating the 200 nm limit is still unexplored. In addition to the above mentioned practical applications, the creation of sub-200 nm surface structures in a high refractive-index nonlinear medium such as LN ($n \sim 2.2-2.4$) is also interesting from a fundamental point of view since they could open the avenue to interesting fundamental phenomena, such as extraordinarily high transmission or polarization-sensitivity effects.[8]

In this letter, we report on the femtosecond laser fabrication of sub-λ/4 holes in a LN crystal by multipulse ablation, with a full control over the hole diameter in the 80–250 nm range. We demonstrate that the presence of the fabricated nanoholes strongly modulates the near-field optical transmission of the LN surface. We show that the near-field transmitted intensity almost vanishes at hole's central position, whereas a significant near-field enhancement is produced at its surroundings. By comparing the measured and three-dimensional finite difference time domain (3D-FDTD) simulated near field maps we found nanometric surface relief as the key factor for the optical contrast mechanism.

The LN samples used in this work were $0.5 \times 1 \times 10$ mm^3 prisms in both x-cut and z-cut orientation. Femtosecond laser ablation was done by using a Spitfire (Spectra Physics) regenerative amplifier generating ~150 fs, linearly polarized pulses at 800 nm wavelength, with a 1 kHz repetition rate. The laser beam was focused onto the LN surface by using an oil immersion Olympus PlanAPO 60X TIRFM microscope objective with a NA of 1.45. The laser beam was expanded and then cut with a pinhole to fit the 5 mm diameter of the objective's back aperture. In order to increase the reproducibility and homogeneity of the obtained holes, we used multipulse ablation so that each sample point was irradiated for 50 ms, with ~50 pulses. The laser power was measured before the objective and was gradually varied between 10 and 100 mW by using a pair of polarisers. Laser polarization was always kept constant, and only the sample was rotated so that polarization was always parallel to the *y* axis of the LN lattice, for both x-cut and z-cut sample orientations. Different holes were written for the same laser power in order to minimize statistical error and confirm the deterministic ablation process. Similar ablation results were obtained for x-cut and z-cut samples. Figure 1(a) shows the specific dependence of the hole diameter on laser pulse energy in a x-cut sample. In this graph dots are experimental data and solid line is the best fit to a $D^2 = \alpha \ln(E/E_{th})$ Beer Law trend, being E and E_{th} the laser pulse and threshold energies, respectively.[9] Error bars depict the observed statistical error which is mainly due to laser power variations. The good agreement between experimental data and a Beer law trend indicates that the hole size is mainly determined by the Gaussian spot ablation threshold mechanism.[9] By taking into

a)Electronic mail: airan.rodenas@uam.es.

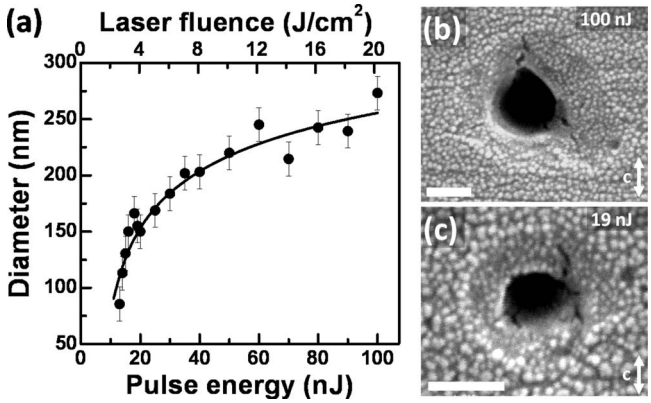

FIG. 1. (a) Hole diameter as a function of laser pulse energy and mean laser fluence. Continuous line corresponds to the fit curve D (nm) $=163.3\sqrt{\ln[E\ (\mathrm{nJ})/8.24]}$. Mean laser fluences were calculated as $F=4E/\pi d_{\mathrm{FWHM}}^2$, where $d_{\mathrm{FWHM}}=\sqrt{2\ln 2}\times 1.22\lambda/\mathrm{NA}\approx 792$ nm. (b) and (c) show high resolution SEM images of holes fabricated with 100 and 19 nJ pulse energies, respectively. Scale bar is 200 nm.

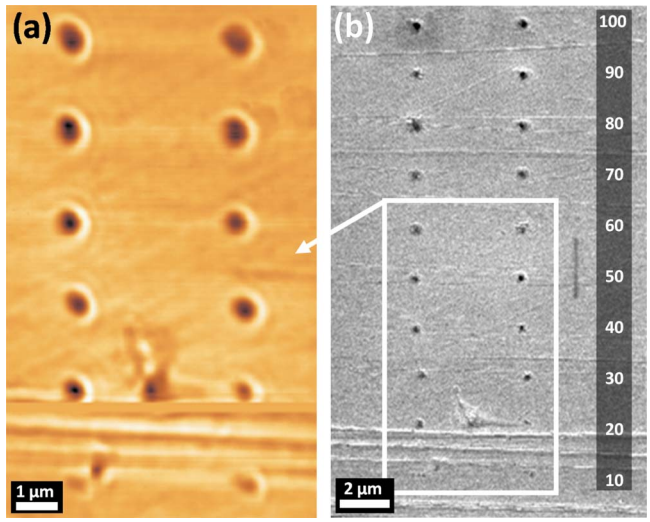

FIG. 2. (Color online) (a) NSOM image of an array of holes ranging from 220 to 80 nm diameter. (b) SEM image of an array of holes indicating the corresponding femtosecond laser pulse fabrication energy in nanojoules.

account the high NA immersion-oil objective transmittance of 70% at 800 nm wavelength, a laser fluence ablation threshold of ~ 1.4 J/cm^2 for 50 pulses was found, in well agreement with our previously reported value of 1.35 J/cm^2 for 100 pulses obtained with low NA nonimmersion objective.[10] This threshold corresponds to laser energy before objective of ~ 10 nJ, while the breakdown of immersion oil was only observed to occur for laser energies above ~ 100 nJ. Data included in Fig. 1(a) demonstrates that it is possible to produce highly symmetric holes with a minimum diameter of 80 nm ($\lambda/10$). Further hole miniaturization is expected to be achieved by using lower laser wavelengths and/or higher NA optics. Figures 1(b) and 1(c) show the scanning electron microscopy (SEM) images of holes obtained with 100 and 19 nJ pulse energies, respectively. The diameter and depth of the obtained structures was also estimated by atomic force microscopy as well as by oblique (45°) SEM measurements. The depth of the fabricated holes was about 15–20 nm for diameters in the range of 150–200 nm, this being in agreement with previous related works.[9]

Figures 2(a) and 2(b) show the NSOM transmission and corresponding SEM image of two rows of holes obtained with different pulse energies (indicated in the figure). The NSOM image was obtained with a Nanonics near-field microscope (MultiView 200 TM) working in noncontact tapping mode using a visible 532 nm continuous wave laser for back illumination of the sample and a ~ 100 nm aperture fiber for near-field collection. The fiber was kept at a constant separation of ≈ 20 nm above the LN surface. From Fig. 2(a) it is clear that, independently on its size, the near-field transmission intensity distribution of an individual hole is constituted by a central shadow core surrounded by a bright inhomogeneous corona. These features are more clearly appreciated in Fig. 3(a), where the experimental NSOM transmission image of a ~ 200 nm diameter hole fabricated with pulse energy of 40 nJ is shown, and also in Fig. 3(c), where the transmission image cross section is given (normalized to the value at normal flat surface away from the hole). From these figures it can be concluded that at the hole center position the near-field intensity is reduced by $\sim 75\%$ of its value outside it, while at its surroundings a near-field transmission ring-shaped enhancement of $\sim 20\%$ is also observed. This high optical contrast being more than two times the optical contrast observed in the NSOM images of air nanoholes fabricated in high-index SiN membranes.[11] The measured field minima at hole position, I_{min}, was observed to follow a decreasing single exponential trend with hole diameter [see inset in Fig. 3(c)]. This allows disregarding possible tip-sample distance fluctuations as a perturbation of our analysis, as no significant change in the exponential trend is observed for holes smaller or higher than the tip diameter (i.e., for conditions in which the NSOM mapping distance with respect to sample's surface would be altered at hole position).

The experimental image in Fig. 3(a) depicts the characteristic near-field light transmission distribution through the nanoholes suggesting the presence of a local near-field confinement in their surroundings, as well as near-field optical inhibition at hole's center. These effects could have two main origins: They could be mainly caused by either the surface ablation relief, creating a nonhomogeneous high-refractive contrast between LN ($n\approx 2.3$) and the air inside the nanohole ($n=1$), and/or by the refractive-index changes created at the nanohole surroundings, as a consequence of the microstructural modifications induced by the fs laser writing process (such as charge separation, lattice strain, densification, or partial amorphization).[10,12] In order to clarify this, simulations of our NSOM experimental conditions were performed with a 3D-FDTD model, assuming an unperturbed LN surface free of density fluctuations and defects (i.e., with a constant refractive index of 2.3), and back-illuminated with a 532 nm wavelength plane wave beam, as depicted in the inset of Fig. 3(c). The near-field intensity was calculated at a constant distance of 20 nm above the LN surface (tip-sample distance in our experimental conditions). Both the experimental and this simulated near-field intensity 2D spatial distributions are shown in Figs. 3(a) and 3(b), respectively. As can be observed, the simulation well reproduces the main features of the experimental measurements: a strong near-field inhibition at hole's position ($\sim 75\%$) and a significant enhancement in its surroundings ($\sim 20\%$). This agreement is also clarified in Fig. 3(c) in which the profiles of the experimental and simulated near-field intensity spatial distributions

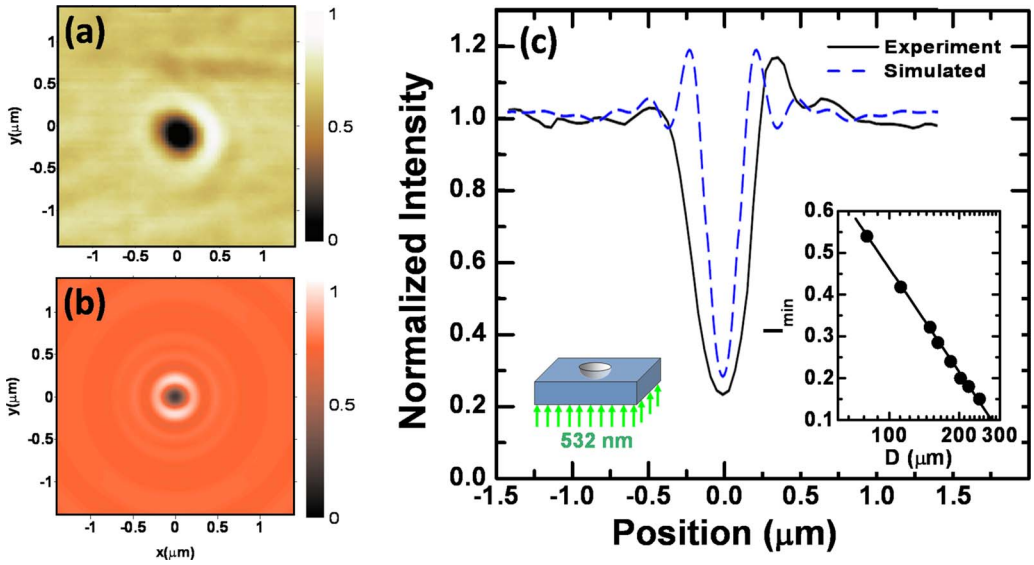

FIG. 3. (Color online) (a) and (b) measured and calculated NSOM images of a 200 nm diameter hole, respectively. (c) measured and simulated NSOM intensity cross-section profiles. Insets show an schematic drawing of the simulated hole, and the measured curve of normalized near-field transmission, I_{min}, as a function of hole diameter.

are plotted (continuous and discontinuous lines, respectively). However, when comparing the intensity profiles of the experimental and simulated images, it is also clear that the ring-shaped bright halo experimentally observed at the hole surroundings is not symmetric, as it is in the simulations. The inhomogeneous bright halo was, in fact, observed to rotate when the NSOM imaging was performed after rotating the sample. This disregards a possible anisotropy of the NSOM aperture as the origin of the inhomogeneous halo. We state that this difference between simulation and experiment could be caused by the intrinsic optical anisotropy of the LN lattice, which was not taken into account in the simulation.

It should also be noted that the experimentally obtained full width at half maximum of the near-field transmission drop off at hole's position is broader than that of the simulation. This discrepancy could most likely be caused by the finite size (~100 nm) of our detecting probe, as similar fiber tip-induced differences between NSOM experimental data and simulations have been reported in other similar systems.[13,14] Yet, the reasonable agreement between experiments and simulation was obtained assuming an unperturbed LN network, this indicating that the main mechanism causing the high near-field optical contrast is the surface relief, leading to a strong refractive-index singularity at hole's position. In this sense, although the presence of refractive-index modifications in the hole's surrounding cannot be disregarded, its contribution to the observed near-field transmission seems to be of a second order level.

In conclusion, we have demonstrated the creation of sub-$\lambda/4$ holes by 800 nm wavelength femtosecond laser ablation in a LN crystal. We have provided experimental evidence that the $\lambda/4$ limit can be beaten, reaching values down to $\lambda/10$. The near-field response of the sub-$\lambda/4$ holes has been found to be characterized by a strong inhibition in the near-field transmission (as large as ~75%) at hole's position, surrounded by a ring-shaped region where an enhancement of up to ~20% is observed. Simulations have well reproduced these main features by assuming a homogeneous hole created in an unperturbed LN network, this indicating surface relief modulation as the main mechanism at the basis of the observed high optical contrast.

This work has been supported by the Spanish Ministerio de Educación y Ciencia (Grant Nos. MAT2004-0334 and MAT2007-64686), by the Universidad Autónoma de Madrid and Comunidad Autónoma de Madrid (Project Nos. MICROSERES-CM and CCG07-UAM/MAT-1861), by the Australian Research Council (ARC) Centre of Excellence for Ultrahigh-bandwidth Devices for Optical Systems (CUDOS), Grant No. CE0348259, and by ARC Discovery (Grant No. DP0665868). A.R. and J.L. contributed equally to this work.

[1]S. Diziain, J. Amet, F. I. Baida, and P. M. Bernal, Appl. Phys. Lett. **93**, 261103 (2008).
[2]G. A. Torchia, C. Mendez, I. Arias, L. Roso, A. Rodenas, D. Jaque, Appl. Phys. B: Lasers Opt. **83**, 559 (2006).
[3]K. Kokkonen, M. Kaivola, S. Benchabane, A. Khelif, and V. Laude, Appl. Phys. Lett. **91**, 083517 (2007).
[4]M. Merano, G. Boyer, A. Trisorio, G. Chériaux, and G. Mourou, Opt. Lett. **32**, 2239 (2007).
[5]F. Korte, J. Serbin, J. Koch, A. Egbert, C. Fallnich, A. Ostendorf and B. N. Chichkov, Appl. Phys. A: Mater. Sci. Process. **77**, 229 (2003).
[6]Y. V. White, X. Li, Z. Sikorski, L. M. Davis and W. Hofmeister, Opt. Express **16**, 14411 (2008).
[7]N. Hartmann, S. Franzka, J. Koch, A. Ostendorf and B. N. Chichkov, Appl. Phys. Lett. **92**, 223111 (2008).
[8]A. Battula, S. Chen, Y. Lu, R. J. Knize and K. Reinhardt, Opt. Lett. **32**, 2692 (2007).
[9]A. P. Joglekar, H. Liu, G. P. Spooner, E. Meyhöfer, G. Mourou and A. J. Hunti, Appl. Phys. B: Lasers Opt. **77**, 25 (2003).
[10]A. Ródenas, J. A. Sanz García, D. Jaque, G. A. Torchia, C. Mendez, I. Arias, and L. Roso, F. Agulló-Rueda, J. Appl. Phys. **100**, 033521 (2006).
[11]A. L. Campillo, W. P. Hsu, G. W. Bryant, Opt. Lett. **27**, 415 (2002).
[12]S. Juodkazis, M. Sudzius, V. Mizeikis, H. Misawa, E. G. Gamaly, Y. Liu, O. A. Louchev, and K. Kitamura, Appl. Phys. Lett. **89**, 062903 (2006).
[13]B. Jia, X. Gan and M. Gu, Opt. Express **13**, 6821 (2005).
[14]B. Jia, X. Gan and M. Gu, Appl. Phys. Lett. **86**, 131110 (2005).